Drug Delivery

DOI: 10.1002/anie.201203339

Photocontrolled Targeted Drug Delivery: Photocaged Biologically Active Folic Acid as a Light-Responsive Tumor-Targeting Molecule**

Nien-Chu Fan, Fong-Yu Cheng, Ja-an Annie Ho, and Chen-Sheng Yeh**

One major problem in current chemotherapy is the drug dosage given to patients. A low dosage of drug is ineffective in the treatment of a tumor, whereas a high dosage of chemotherapeutics is intolerable for patients due to toxicity and side effects. Therefore a new design for anticancer drugs is desirable to increase the local effective therapeutic concentration. Two promising strategies are primed to achieve this goal; one is to construct a stimuli-responsive drug delivery system for controlled drug release and the other is to formulate a system for actively targeting the delivery of the therapeutic agent. Both approaches can minimize adverse effect of cytotoxic drugs and improve the therapeutic efficacy of conventional pharmaceuticals. Active targeting that uses specific ligands including monoclonal antibodies, peptides, and aptamers that bind to specific proteins or surface antigens overexpressed on cancer cells is a practical and attractive way to enhance the local control of therapeutics. For example, folic acid (FA), a low-molecular-weight vitamin, plays an essential role in cell survival and binds with high affinity to the folate receptor (FR), a membrane-anchored protein. The bound folate and folate conjugates enter cells through receptor-mediated endocytosis.[1] It has been found that the FR is overexpressed on cancer cell surfaces and served as a tumor marker.[1b,2] For example, the upregulated FR overexpression occurs in 82% of ovarian carcinoma. Thus, exploitation of FA as a targeting ligand has been intensively investigated for folate-targeted cancer therapeutics.[1,2b,3] However, the number of FRs expressed on the cell surfaces varies for different cancer cells, thus limiting the delivery capacity of FR endocytosis, for example, a moderate to low frequency of FR expression is found in lung (66%, non-small-cell), endometrium (64%), thyroid (48%), breast (29%), and lung (25%, small-cell) carcinoma.[4] Furthermore, significant FR expression occurs in normal kidney cells and also appears in activated macrophages that are present during inflammatory diseases in a patient without malignant mass.[4,5]

Light is an external stimulus and provides a great benefit to release a drug at a desired time and place; this control is considered crucial to boost drug efficacy in cancer treatment. Photomodulation is a niche technique in chemical and biomedical tools. Photocaging is a method, where a molecule is derivatized with a photolabile protecting group, resulting in a biologically inert caged molecule.[6] Illumination with light to liberate a caging group and activate cytotoxic drugs provides spatial, temporal, and concentration-dependent control in drug delivery, thereby resulting in enhanced local toxicity in the specific irradiated tumor area. Therefore, the innocuous antitumor drugs (prodrugs) are developed and delivered to cells and tissues, where they are unmasked to their active forms.[7] In recent studies, the species for photocontrolled targeting were constructed by the introduction of photocaging groups on peptides.[8] The photolabile 4,5-dimethoxy-2-nitrobenzyl group was either attached to the tyrosine segment of the peptide YIGSR or on the cell-penetrating peptides with the KRRMKWKK sequence. Inspired by this elegant approach, we thought it could be potentially adopted to improve specific adsorption and cellular uptake for tumor-homing agents, for example, folic acid, and further be applied to nanocarriers for intracellular drug delivery.

Herein, we report a proof-of-concept design of photocaged folate nanoconjugates that selectively target cancer cells upon irradiation with UV light (Figure 1). The folic acid is masked by a photocleavable *o*-nitrobenzyl (ONB) group through covalently binding to α- and γ-carboxylate groups, which interact with FRs on the cell surface.[9] We first synthesized a caged folate molecule and examined its targeting specificity. Subsequently the nanoconjugates, being Au nanoparticles with caged folate molecules attached on the surface, were fabricated to observe the internalization of Au nanoparticles into cancer cells when upon photoactivation the caging groups on the folate groups of the Au nanoconjugates were removed. Then, light-activated targeting and intracellular drug delivery were demonstrated using biodegradable PLGA@lipid hybrid nanoparticles (PLGA = poly(D,L-lactide-*co*-glycolide)) encapsulating the drug paclitaxel (Taxol). Light illumination triggered uncaging and activated

[*] Prof. C.-S. Yeh
Department of Chemistry, Center for Micro/Nano Science and Technology, and Advanced Optoelectronic Technology Center
National Cheng Kung University
Tainan 701, Taiwan
E-mail: csyeh@mail.ncku.edu.tw
Prof. J.-A. A. Ho
Department of Biochemical Science and Technology
National Taiwan University
Taipei 10167 (Taiwan)
N.-C. Fan,[+] Prof. J.-A. A. Ho
Department of Chemistry, National Tsing Hua University
Hsinchu 30013 (Taiwan)
E-mail: jaho@ntu.edu.tw
Prof. F.-Y. Cheng[+]
Institute of Oral Medicine, National Cheng Kung University
Tainan 701 (Taiwan)
[+] These authors contributed equally to this work.

[**] This work was supported by the National Science Council of Taiwan. (NSC 100-2627-M-006-007, NSC 100-2119-M-006-021, and 98-2113-M-002-025-MY3).
Supporting information for this article is available on the WWW under http://dx.doi.org/10.1002/anie.201203339.

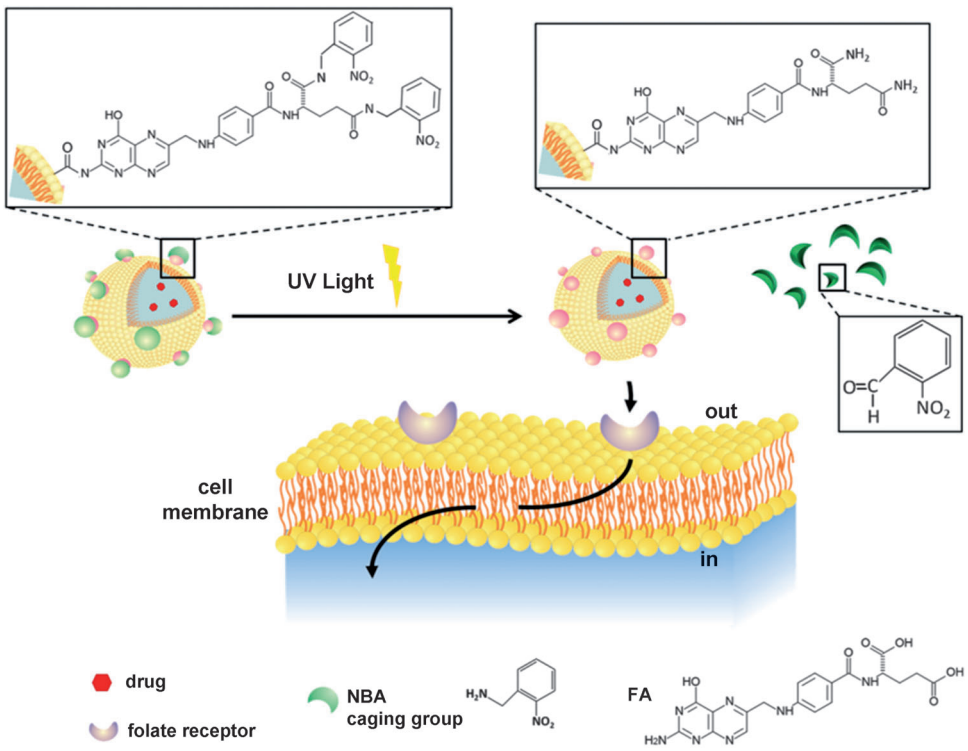

Figure 1. The photocaged folate nanoconjugates are activated by irradiation to remove the caging groups, and then to target cancer cells. NBA = 2-nitrobenzylamine.

FA for targeting. The FA-mediated cellular internalization allowed degradable PLGA@lipid nanoparticles to release Taxol, thereby causing a higher cytotoxicity to the target cells than the unactivated nanoparticles.

Prior to the conjugation of FA to the nanoparticles, caging and photouncaging were evaluated using the bare FA molecule. The carboxylate groups of FA can be recognized by folate receptors on the cell surface; in particular the α-carboxylate moiety exhibits a high affinity towards the FR. Hence, the carboxylate groups of FA were modified with amino groups of the cage molecule 2-nitrobenzylamine (NBA) to form amide bonds through (1-ethyl-3-(3-dimethylaminopropyl)carbodiimide hydrochloride/*N*-hydroxysuccinimide (EDC/NHS) chemistry. The caged folate can be readily dissolved in H_2O. ^1H NMR spectroscopy (Figure S1 in the Supporting Information) was performed at different FA/NBA mole ratios (loading amount ratio). The multiplet peaks displayed in the range of $\delta = 7$–8.5 ppm chemical shift attribute to aromatic rings of NBA conjugated with FA. The appearance of a peak at $\delta = 12.8$ ppm is an indicator for the presence of carboxylate groups. As the FA/NBA mole ratio was raised to 1:5 (Figure S1 c in the Supporting Information), the carboxylate signal disappeared, thereby indicating both -COOH groups were completely masked by NBA. In fact, a 1:3 ratio was sufficient to cage both carboxylate moieties. The ONB chromophore has a UV absorption maximum around 265 nm (Figure S2 in the Supporting Information) and undergoes photolytic cleavage upon UV illumination. The fully caged folate was used after choromatographic purification. Photolysis was performed using a Hg lamp (1.06 mW cm^2) for 20 min irradiation with a distance fixed at 3 cm between optical fiber head and target throughout the experiments. Upon light irradiation, UV/Vis absorption showed a decrease in intensity at 265–270 nm along with a growing peak at 285 nm. The spectral change is due to the cleavage of the ONB group and formation of 2-nitrobenzaldehyde. The broad band appearing at 360–380 nm corresponds to FA. Contrarily, no photocleavage occurred when the fully caged folate was subjected to irradiation with a 633 nm continuous-wave diode laser.

Cellular fluorescence imaging was conducted to evaluate whether or not the caged folate can still be recognized by the FR and if the uncaged folate with two primary amide (α and γ-(CO)NH_2) groups, which are formed after the photocleavage reaction, keeps its affinity to the FR. The opposite terminus of folic acid contains an amino group that was covalently bound to the fluorescent dye FITC (FITC = fluorescein 5(6)-isothiocyanate) through formation of an amide bond using an EDC/NHS reaction. By following the same aforementioned protocol, the caged folate/FITC conjugates were obtained by the protection of two carboxylate groups of FA using the NBA caging group. The folate/FITC, caged folate/FITC (no irradiation), and caged folate/FITC conjugates (with light irradiation) were examined using folate-receptor-positive KB cells (Figure S3 in the Supporting Information). Those three conjugates were individually incubated with KB cells with or without light exposure at 4 °C for 20 min. The cancer cell targeting was performed at 4 °C because the endocytosis could be dramatically reduced or inhibited at this temperature. As expected, the uncaged folate/FITC conjugate effectively targeted KB cells exhibiting green fluorescence (Figure S3 a, d in the Supporting Information). The caged folate/FITC conjugate showed no targeting (Figure S3 b, e in the Supporting Information), while photolysis of caged folate/FITC conjugates brightened cells again (Figure S3 c, f in the Supporting Information). These results support that caging -COOH groups with NBA effectively alters FA affinity to the cell surface receptors, and the selective binding of FA to the FR can be resumed by the photoactivation approach.

Subsequently, the caged folate design was applied to Au nanoparticles (Scheme 1). The citrate-reduction method was used to prepare 13 nm Au nanoparticles (NPs).[10] The Au NPs were modified with mercaptopropionic acid (MPA), then the exposed -COOH groups were conjugated to FA through amide formation, and subsequently the NBA caging groups

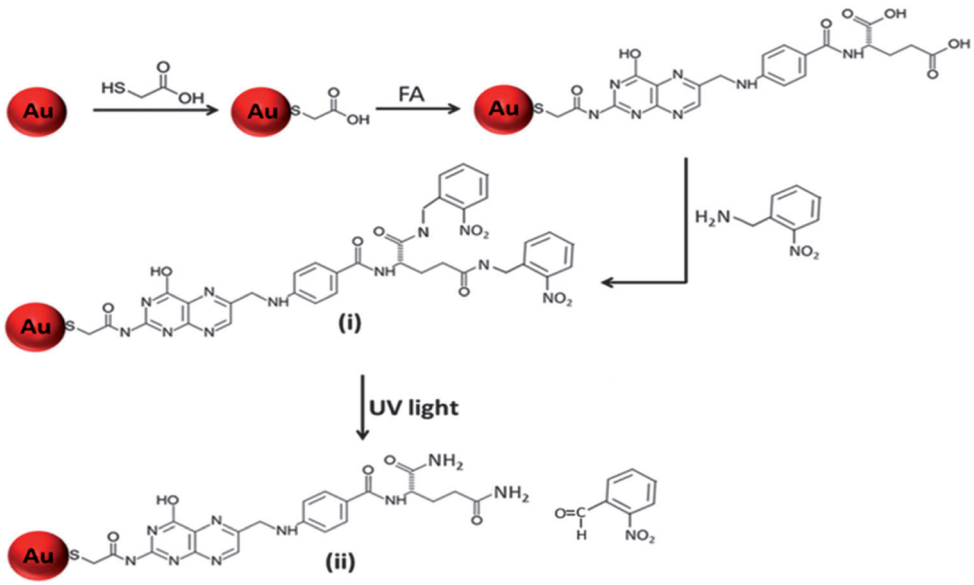

Scheme 1. Preparation of caged folate/Au nanoconjugates (i) and cleavage of the caging group under light irradiation to give the nanoconjugate with the free FA (ii).

were attached to mask the FA. The transmission electron microscopy (TEM) images in Figure S4 in the Supporting Information show the dispersed Au nanoconjugates. Measurements of the zeta-potential indicate the surface charges as −27.1 mV on as-prepared Au NPs, −25.5 mV on folate/Au nanoconjugates, and 5.4 mV on caged folate/Au nanoconjugates. Figure S5 in the Supporting Information shows the UV/Vis spectra for Au NPs, folate/Au and caged folate/Au nanoconjugates. The surface plasmon characteristic peak of Au at 520 nm shifted slightly to red after conjugation to FA and NBA molecules on the surface. Both folate/Au and caged folate/Au nanoconjugates show an additional band located around 280–300 nm, attributing to aromatic moieties of FA and NBA molecules. A band near 360 nm originates from FA. FTIR spectra provide additional evidence for folic acid modification of the Au NPs (Figure S6 in the Supporting Information). Since the characteristic peak of the aromatic groups of the NBA cage molecule overlaps with those of FA, FTIR spectroscopy cannot be used to identify the presence of NBA caging on folate/Au nanoconjugates. The amount of immobilized FA was measured from the decrease in intensity of the UV/Vis absorbance of FA that was left in the supernatants and calculated using a calibration curve derived from the FA concentration. From the result we estimate that a maximum number of approximately 2274 FA molecules are attached on a single Au NP. Since each FA molecule contains two -COOH groups, we found that approximately 80 % of the -COOH groups is the highest value that can be caged by NBA in the case that approximately 2274 FA molecules are attached to one Au NP. This incomplete functionalization is presumably due to the steric hindrance that results from full coverage with FA, thus preventing complete conjugation of NBA. Photouncaging was examined using the absorbance peak of the photocleavage product 2-nitrobenzaldehyde appearing at 285 nm. The caged folate/Au nanoconjugates were dispersed in phosphate-buffered saline (PBS) buffer (pH 7.4) and exposed to light as a function of illumination time (Figure S7 in the Supporting Information). The peak corresponding to 2-nitrobenzaldehyde increases with prolonged exposure time, while no signal at 285 nm was detected in the absence of light. Reverse-phase HPLC was also conducted to observe the cleaved 2-nitrobenzaldehyde product after irradiation of caged folate/Au nanoconjugates (Figure S8 in the Supporting Information). 2-Nitrobenzaldehyde appeared at a retention time of 5.6 min. After 20 min exposure a photouncaging efficiency of approximately 69 % was estimated based on the difference in the integrated peak area when compared with the amount of 2-nitrobenzaldehyde that would be expected if all the NBA groups on the caged folate had been removed.

Figure 2 shows the cancer cell (KB cells) targeting studies conducted at 4 °C. KB cells were collected and subjected to inductively coupled plasma atomic emission spectroscopy (ICP-AES) measurements to determine the number of Au particles that were taken up by the cells. The folate/Au nanoconjugates readily attached to malignant cells, whereas the affinity of caged folate/Au nanoconjugates to the folate receptor was significantly reduced. Because approximately 80 % of the -COOH groups of FA were blocked by NBA (in the case of ca. 2274 FA per Au NP), the residual unmasked carboxylate moieties could have shown a low binding activity, thus resulting in the binding of some Au NPs to cells when treated with caged folate/Au nanoconjugates. When the number of FA molecules per Au NP was decreased to approximately 810 to reduce the steric hindrance as mentioned earlier, the amount of caged folate/Au nanoconjugates that was taken up by KB cells dropped to approximately 56 % relative to those of Figure 2 with 2274 FA molecules per Au NP. Upon light irradiation, the number of cells that took up Au NPs apparently raised. The uncaging efficiency of approximately 69 % could possibly contribute to the observed difference in number of particles on cells between folate/Au and caged folate/Au nanoconjugates (with light irradiation). Photocontrolled targeting experiments were further carried out on malignant lung A549 cells, displaying low FR expression, and the results indicated much less Au NP targeting to FR-negative A549 cells than to KB cells (Figure S9 in the Supporting Information). The MTT assay (MTT = 3-(4,5-dimethylthiazol-2-yl)-2,5-diphenyltetrazolium bromide) was used to assess cell viability for Au NPs, folate/Au and caged folate/Au nanoconjugates. For the experiments without irradiation, KB cells were incubated with different concentrations of Au in 96-well plates for 24 h and subjected

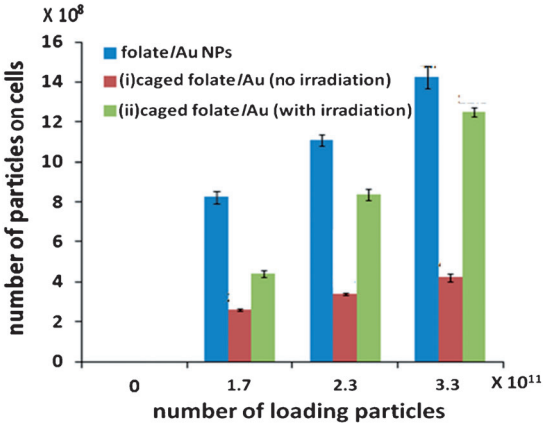

Figure 2. Targeting cells with folate/Au nanoconjugates and caged folate/Au nanoconjugates at 4 °C for 20 min. Different numbers of folate/Au and caged folate/Au nanoconjugates were individually incubated with KB cells. For the caged folate/Au nanoconjugates exposed to light, the experiments were performed at 4 °C for 20 min irradiation. Photolysis was performed using an Hg lamp (1.06 mW cm^2) with the distance fixed at 3 cm between optical fiber head and target place. After 20 min illumination period, the unbound nanoparticles were removed first, and then the number of Au nanoparticles that resided on cells were determined by ICP-AES measurements. The numbers of loaded caged folate/Au nanoconjugates 1.7×10^{11}, 2.3×10^{11}, and 3.3×10^{11} correspond to Au ion concentrations of 50, 75, and 100 μg mL^{-1}, respectively. (i) and (ii) correspond to the conjugates shown in Scheme 1.

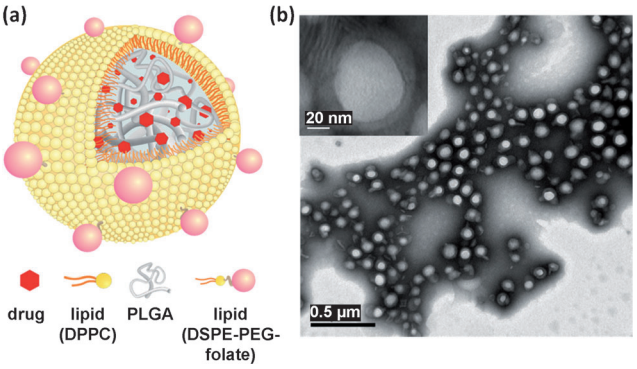

Figure 3. a) Schematic view of a folate/PLGA@lipid nanoconjugate. b) TEM image of the PLGA@lipid hybrid nanoparticles containing no paclitaxel drug observed using negative staining with phosphotungstic acid (0.1 % *w*/*v* in water). The average diameter of the PLGA core is around 71 nm. Inset shows an enlarged nanoparticle.

to MTT measurements. For the experiments with light exposure, the cells were first irradiated at 4 °C for 20 min and then cultured at 37 °C for additional 24 h. No significant drop in cell viability (> 90 %) was observed for all nanoparticle and nanoconjugate samples (Figure S10 in the Supporting Information). No cell damage was seen when KB cells alone were irradiated.

Next, the application of the caged folate for intracellular drug delivery was examined by using a biodegradable PLGA@lipid hybrid nanoparticle. PLGA@lipid NPs encapsulating Taxol drug were prepared by self-assembly of PLGA (MW: 35 000–65 000 Da), 1,2-dipalmitoyl-*sn*-glycero-3-phosphocholine (DPPC; MW: 734 Da), and 1,2-distearoyl-*sn*-glycero-3-phosphoethanolamine-*N*-[carboxy(polyethylene glycol)-2000] (DSPE-PEG(2000)carboxylic acid) using a single-step nanoprecipitation approach. The PLGA polymer alone normally self-assembles into a spherical NP with a hydrophilic surface and a hydrophobic core.[11] Herein, it is thought that the hydrophobic segment of the PLGA structure has two functions: to encapsulate the hydrophobic Taxol and to self-assemble with phospholipids. DPPC, a so-called lecithin, is a phospholipid that has been commonly used for the formulation of liposomes and lipid layers.[12] The PLGA@-lipid NP consists of phosphate headgroups of phospholipids facing outward and PLGA remaining in the core (Figure 3a).[13] Both DPPC and DSPE-PEG carboxylic acid (DSPE-PEG carboxylic acid/DPPC = 0.4 % in amount) contribute to the lipid layer. Using EDC/NHS-mediated crosslinking the DSPE-PEG carboxylate group was coupled to a folate moiety. Prior to the folate conjugation, the zeta potential of the hybrid nanoparticles was determined to be −24.0 mV with an average diameter of approximately 137 nm from dynamic light scattering (DLS). PLGA@lipid NPs (without Taxol encapsulated) were also imaged by TEM (Figure 3b). Different contrast was seen between the denser PLGA nanoparticle core and the lipid layer. Based on the TEM image, the PLGA core has a size of approximately 71 nm and the lipid shell a thickness of approximately 2.5 nm, which is consistent with half of a lipid-bilayer length (ca. 5.4 nm).[14] The amount of phospholipids on the surface of PLGA NPs was determined by a modified Bartlett phosphorus assay,[15] resulting in approximately 1.2×10^{-4} mmol of phospholipid (DPPC) molecules on the surface of 1 mg PLGA NPs (Figure S11 in the Supporting Information).

After formulation of PLGA@lipid NPs containing Taxol, FA was anchored on the surface by conjugation with the carboxylate groups of the DSPE-PEG carboxylic acid; the zeta potential and average hydrodynamic diameter of the resulting NPs were −28.3 mV and 173 nm, respectively. The number of FA molecules in 1 mg of folate/PLGA@lipid nanoconjugates is estimated to be 1.3×10^{15}. HPLC measurements also determined a maximum amount of 1.7 μg Taxol encapsulated per 1 mg of folate/PLGA@lipid nanoconjugates. The in vitro release profile of Taxol from folate/PLGA@lipid nanoconjugates was determined in PBS (pH 7.4) at 37 °C (Figure S12 in the Supporting Information) and monitored by HPLC. The initial drug release profile of folate/PLGA@lipid nanoconjugates loaded with Taxol included a burst release of approximately 31 % within eight hours, followed by a slow release to gradually approach 62 % after 72 h. The release of Taxol was due to entrapped Taxol diffusing into PBS during PLGA degradation.

At last, the NBA cage molecules were conjugated onto the anchored folate moieties by using the aforementioned process, to form caged folate/PLGA@lipid nanoconjugates encapsulating Taxol for photocontrolled targeted intracellular drug delivery. KB cells were individually treated with free Taxol, folate/PLGA@lipid NPs, folate/PLGA@lipid nanoconjugates containing Taxol, and caged folate/PLGA@lipid nanoconjugates containing Taxol, and subjected to MTT assays (Figure 4). The same procedure as for the Au NPs was used for the caged folate/PLGA@lipid nanoconjugates con-

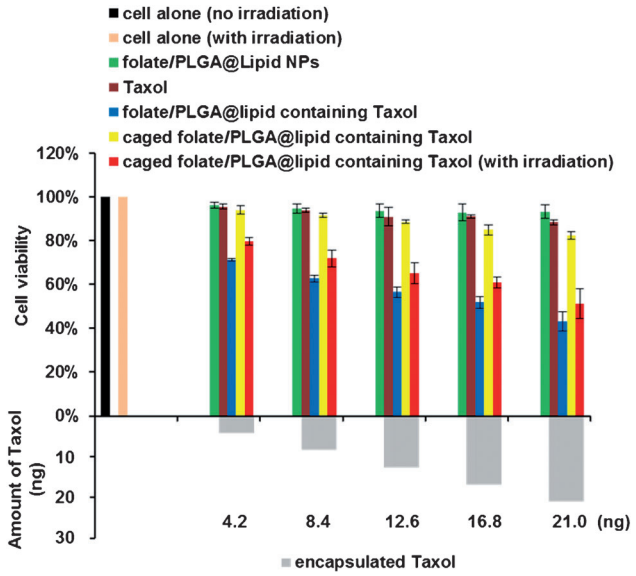

Figure 4. Cell viability studies of KB cells incubated individually with the listed reagents. A series of PLGA@lipid dosages (2.5, 5.0, 7.5, 10, and 12.5 μg) was used, with these dosages corresponding to 4.2, 8.4, 12.6, 16.8, and 21 ng of Taxol encapsulated in PLGA@lipid nanoconjugates, respectively. The gray columns represent the groups containing a specific amount of Taxol. For the experiments with the caged folate/PLGA@lipid nanoconjugates containing Taxol that were exposed to light, the cells were first irradiated at 4 °C for 20 min, and then cultured at 37 °C for additional 24 h. Photolysis was performed using a Hg lamp (1.06 $mW cm^{-2}$) with a distance fixed at 3 cm between optical fiber head and target place.

taining Taxol; thus cells were irradiated at 4 °C for 20 min, and then cultured at 37 °C for additional 24 h. If the experiment was performed without irradiation, the cells were incubated for 20 min at 4 °C followed by incubation at 37 °C for 24 h. Cell viability remains above 90 % at different concentrations of PLGA@lipid NPs. The caged folate/PLGA@lipid nanoconjugates (no irradiation) showed the cell viability remains high and the survival rate is up to approximately 83 % for the group with 21 ng of encapsulated Taxol. However, the cell viability decreased to approximately 51 % when the caged folate/PLGA@lipid nanoconjugates encapsulating 21 ng of Taxol were exposed to irradiation. In fact, the caged folate/PLGA@lipid nanoconjugates (with irradiation) exerted a comparable effect on cell damage as the folate/PLGA@lipid nanoconjugates (no caging) in a series of PLGA@lipid dosages (2.5, 5.0, 7.5, 10, and 12.5 μg of encapsulated Taxol). The important outcome is that the drug toxicity elevates under irradiation. Moreover, the cells treated with 21 ng of free Taxol showed approximately 89 % cell viability. It is noted that the encapsulated Taxol in PLGA@lipid NPs was not completely released after 24 h incubation.

In conclusion, we report that caging and photouncaging can be applied to FA to potentially improve its targeting specificity. Intracellular drug delivery performance also demonstrated that the cytotoxicity of the used anticancer drug increased upon light irradiation. A major concern is the use of the UV light emitted by the Hg lamp to trigger uncaging; this light has a poor tissue penetration, which limits in vivo applications of this approach to the body. However, the UV light source can be alternatively replaced by a near-infrared light, along with the utilization of a two-photon photoactivation caging molecule or a lanthanide-based upconversion nanoparticle. An upconversion luminescent nanoparticle can convert low energy of near-infrared wavelength to higher-energy radiation (UV light) through multiple absorption or energy transfer.

Received: May 1, 2012
Published online: July 25, 2012

Keywords: cytotoxicity · drug delivery · nanoparticles · photocaging · prodrugs

[1] a) J. Sudimack, R. J. Lee, *Adv. Drug Delivery Rev.* **2000**, *41*, 147–162; b) B. A. Kamen, A. K. Smith, *Adv. Drug Delivery Rev.* **2004**, *56*, 1085–1097; c) A. R. Hilgenbrink, P. S. Low, *J. Pharm. Sci.* **2005**, *94*, 2135–2146.
[2] a) J. F. Ross, P. K. Chaudhuri, M. Ratnam, *Cancer* **1994**, *73*, 2432–2443; b) H. Elnakat, M. Ratnam, *Adv. Drug Delivery Rev.* **2004**, *56*, 1067–1084; c) S. D. Weitman, R. H. Lark, L. R. Coney, D. W. Fort, V. Frasca, V. R. Zurawski Jr., B. A. Kamen, *Cancer Res.* **1992**, *52*, 3396–3401.
[3] a) S. Dhar, Z. Liu, J. Thomale, H. Dai, S. J. Lippard, *J. Am. Chem. Soc.* **2008**, *130*, 11467–11476; b) Y. Zhu, Y. Fang, S. Kaskel, *J. Phys. Chem. C* **2010**, *114*, 16382–16388; c) Z. Zhang, J. Jia, Y. Lai, Y. Ma, J. Weng, L. Sun, *Bioorg. Med. Chem.* **2010**, *18*, 5528–5534.
[4] W. Xia, P. S. Low, *J. Med. Chem.* **2010**, *53*, 6811–6824.
[5] C. Muller, F. Forrer, R. Schibli, E. P. Krenning, M. de Jong, *J. Nucl. Med.* **2008**, *49*, 310–317.
[6] a) G. Mayer, A. Heckel, *Angew. Chem.* **2006**, *118*, 5020–5042; *Angew. Chem. Int. Ed.* **2006**, *45*, 4900–4921; b) G. C. Ellis-Davies, *Nat. Methods* **2007**, *4*, 619–628; c) H. M. Lee, D. R. Larson, D. S. Lawrence, *ACS Chem. Biol.* **2009**, *4*, 409–427.
[7] a) Z. Zhang, H. Hatta, T. Ito, S. Nishimoto, *Org. Biomol. Chem.* **2005**, *3*, 592–596; b) A. Momotake, N. Lindegger, E. Niggli, R. J. Barsotti, G. C. Ellis-Davies, *Nat. Methods* **2006**, *3*, 35–40; c) C. P. McCoy, C. Rooney, C. R. Edwards, D. S. Jones, S. P. Gorman, *J. Am. Chem. Soc.* **2007**, *129*, 9572–9573; d) S. S. Agasti, A. Chompoosor, C. C. You, P. Ghosh, C. K. Kim, V. M. Rotello, *J. Am. Chem. Soc.* **2009**, *131*, 5728–5729; e) S. K. Choi, T. Thomas, M. H. Li, A. Kotlyar, A. Desai, J. R. Baker Jr., *Chem. Commun.* **2010**, *46*, 2632–2634.
[8] a) T. Dvir, M. R. Banghart, B. P. Timko, R. Langer, D. S. Kohane, *Nano Lett.* **2010**, *10*, 250–254; b) Y. Shamay, L. Adar, G. Ashkenasy, A. David, *Biomaterials* **2011**, *32*, 1377–1386.
[9] S. Wang, R. J. Lee, C. J. Mathias, M. A. Green, P. S. Low, *Bioconjugate Chem.* **1996**, *7*, 56–62.
[10] K. C. Grabar, R. G. Freeman, M. B. Hommer, M. J. Natan, *Anal. Chem.* **1995**, *67*, 735–743.
[11] a) F. Y. Cheng, S. P. Wang, C. H. Su, T. L. Tsai, P. C. Wu, D. B. Shieh, J. H. Chen, P. C. Hsieh, C. S. Yeh, *Biomaterials* **2008**, *29*, 2104–2112; b) F. Y. Cheng, C. H. Su, P. C. Wu, C. S. Yeh, *Chem. Commun.* **2010**, *46*, 3167–3169.
[12] a) J. A. Ho, L. C. Wu, M. R. Huang, Y. J. Lin, A. J. Baeumner, R. A. Durst, *Anal. Chem.* **2007**, *79*, 246–250; b) J. A. Ho, T. Y. Kuo, L. G. Yu, *Anal. Chim. Acta* **2012**, *714*, 127–133.
[13] L. Zhang, J. M. Chan, F. X. Gu, J. W. Rhee, A. Z. Wang, A. F. Radovic-Moreno, F. Alexis, R. Langer, O. C. Farokhzad, *ACS Nano* **2008**, *2*, 1696–1702.
[14] D. Uhríková, N. Kucerka, J. Teixeira, V. Gordeliy, P. Balgavy, *Chem. Phys. Lipids* **2008**, *155*, 80–89.
[15] G. R. Bartlett, *J. Biol. Chem.* **1959**, *234*, 466–468.

